Arthrodesis of the equine proximal interphalangeal joint: a biomechanical comparison of 2 different LCP systems

DOI 10.1055/a-1067-3819
Tierärztliche Praxis Großtiere/Nutztiere 2020; 48: 25–34

Publishing House and Copyright:
© 2020 by
Georg Thieme Verlag KG
Rüdigerstraße 14
70469 Stuttgart
ISSN 1434-1220

Thieme

Arthrodesis of the equine proximal interphalangeal joint: a biomechanical comparison of 2 different LCP systems

Application of an axial locking compression plate and 2 abaxial transarticular cortical screws

Arthrodese des proximalen Interphalangealgelenks beim Pferd: biomechanischer Vergleich von 2 unterschiedlichen LCP-Systemen

Verwendung einer axialen Verriegelungsplatte und zweier abaxialer transartikulärer Kortikalisschrauben

Authors

Aleksandar Vidović[1], Dorothea Jansen[1], Stefan Schwan[2], Alexander Goldstein[2], Christopher Ludtka[3], Walter Brehm[4]

Institutes

1 Equine Clinic St. Georg, Trier, Germany
2 Fraunhofer Institute for Microstructure of Materials and Systems IMWS, Halle, Germany
3 University of Tennessee Health Science Center, Memphis, TN, USA
4 Clinic for Horses, Faculty of Veterinary Medicine, University of Leipzig, Leipzig, Germany

Schlüsselwörter

Pferd, Krongelenk, Krongelenkfusion, Osteosynthese, PIP-LCP, ALPS

Key words

Horse, PIP joint, PIP joint fusion, osteosynthesis, PIP plate, ALPS

received 27.08.2019
accepted 29.10.2019

Bibliography

DOI https://doi.org/10.1055/a-1067-3819
Tierarztl Prax Ausg G Grosstiere Nutztiere 2020; 48: 25–34

ISSN 1434–1220

Correspondence address

Aleksandar Vidović
Equine Clinic St. Georg
Metternichstrasse 9
54292 Trier, Germany
vidovic@pferdeklinik-trier.de

ZUSAMMENFASSUNG

Gegenstand und Ziel Vergleich von mechanischer Stabilität und chirurgischer Handhabung von 2 Verriegelungsplatten-Systemen (ALPS-20, Kyon und PIP-LCP, Synthes) für die Arthrodese des proximalen Interphalangealgelenks beim Pferd.

Material und Methoden Für diese Ex-vivo-Studie standen 6 Beinpaare von adulten Warmblutpferden zur Verfügung, die aus einem nicht orthopädischen Grund euthanasiert wurden. Als chirurgische Technik für die Krongelenksarthrodese wurde eine axial angebrachte Verriegelungsplatte in Kombination mit 2 abaxialen transartikulären 4,5-mm-Kortikalisschrauben gewählt. Zur Fixation der ALPS-20-Platte dienten 3 monokortikal eingesetzte selbstschneidende 6,4-mm-Verriegelungsschrauben mit einer Länge von 28 mm. Die PIP-LCP wurde mit 3 bikortikalen Schrauben implantiert: 2 5,0-mm-Verriegelungsschrauben im proximalen und distalen Plattenloch und eine 4,5-mm-Kortikalisschraube im mittleren Loch. Die mechanische Testung der beiden Präparat-Implantat-Konstrukte erfolgte mit einer servohydraulischen Anlage bei einmaliger uniaxialer Belastung (Testgeschwindigkeit 50 mm/s, Belastungsamplitude 80 mm). Zur Dokumentation der Implantatdeformationen wurden alle Implantate sowohl nach der Implantierung als auch nach der biomechanischen Testung einer CT-Untersuchung auf Deformationen unterzogen. Anhand der resultierenden Belastung-Verlagerung-Kurven wurden Fließpunkt, Steifheit und maximale Belastung für jedes System berechnet. Zur Überprüfung der Messwerte auf statistisch signifikante Unterschiede ($p < 0,05$) zwischen den beiden Plattensystemen diente eine einfaktorielle Varianzanalyse (Tukey-Test). Statistische Power ergab sich für die Parameter Fließkraft, Steifheit und maximale Belastung.

Ergebnisse Die mechanischen Eigenschaften der beiden Verriegelungsplatten-Systemen unterschieden sich in Bezug auf Fließpunkt, Steifheit und maximale Belastung statistisch nicht signifikant ($p > 0,05$). Bei ALPS-20-Implantaten wurden weder nach der Implantierung noch nach der Testung Deformationen festgestellt. Im Gegensatz dazu zeigten die PIP-LCPs Deformationen in der Längsachse schon zum Zeitpunkt der Implantation, nach dem Festziehen der Schraube im mittleren

Plattenloch sowie bei der biomechanischen Testung. Nach der biomechanischen Testung wiesen 4 Platten Längsachsen-Biegungen zwischen 3,1° und 7,0° auf, in 2 Fällen kam es zu einem totalen Versagen.

Schlussfolgerung und klinische Relevanz Die beiden Systeme wiesen vergleichbare mechanische Eigenschaften in Bezug auf Fließpunkt, Steifheit und maximale Belastung auf. Somit sollte das ALPS-20 für die Krongelenksarthrodese beim Pferd als gute Alternative zu dem PIP-LCP-System in Betracht gezogen werden.

ABSTRACT

Objective This study compares the mechanical stability and surgical usability of 2 locking plate systems (Kyon ALPS-20 and Synthes PIP-LCP system) for arthrodesis of the equine proximal interphalangeal joint (PIJ).

Material and methods The experimental ex vivo study included 6 pairs of cadaver distal limbs (n = 12). All specimens were derived from Warmblood horses of various ages that were euthanized for non-orthopedic reasons. Of the 12 limbs collected, 3 left and 3 right distal limb specimens were randomly assigned to each system for implantation. Two abaxial 4.5-mm cortical screws were inserted transarticularly in all cases. Both systems were implanted according to the manufacturer's instructions with the plates placed centrally between the 2 transarticular screws. The ALPS-20 systems were implanted using Kyon B-6.4-mm monocortical locking screws in all positions. The LCP systems were implanted axially using 2 Synthes 5-mm locking screws in the proximal and distal positions, with a standard 4.5-mm cortical screw inserted in the middle position. All constructs underwent CT-scans after implantation and biomechanical testing to detect implant deformation. Uniaxial mechanical loading was applied via a servo-hydraulic test system at a test speed of 50 mm/s, up to a maximum displacement of 80 mm. The resulting load-displacement curves were used to calculate yield point, stiffness, and maximum force for each construct. The measured values were evaluated for statistical significance ($p < 0.05$) between the 2 plate systems via one-factor ANOVA (Tukey test). The statistical power was verified for yield force, stiffness, and maximum load.

Results No statistically significant differences between the 2 preparation groups were calculated across all of the measured parameters ($p > 0.05$). The ALPS system implants showed no signs of deformation, either in the plates or the screws. In contrast, the LCP demonstrated visible deformation, which had already occurred at the time of implantation from the tightening of the middle screw, as well as during the subsequent testing of the implants. After biomechanical testing, deformations ranging between 3.1° and 7.0° were measured in 4 LCPs. A total implant failure was observed for 2 LCPs.

Conclusion and clinical relevance Both systems demonstrated comparable mechanical properties in the present study's ex vivo test model for equine PIJ arthrodesis. As such, the Kyon ALPS-20 may be a good alternative to the Synthes LCP for equine PIJ arthrodesis.

Introduction

Arthrodesis in horses is most often performed and reported in regard to the proximal interphalangeal joint (PIJ) [1][2][3][4][5]. The unique biological and behavioral characteristics of horses necessitate specific surgical objectives when performing PIJ arthrodesis. First, a secure connection between the proximal phalanx (P1) and middle phalanx (P2) must be established using a suitable implant and an optimal surgical technique for successful joint fusion [3][4][5][6][7]. In addition, the implants and their anchor points in the bone must also withstand the inherent cyclic stresses until P1 and P2 fuse; i. e., until the process of ankylosis is completed.

There are numerous surgical fixation methods that can be performed to achieve PIJ arthrodesis. Initially, 2–3 cortical screws of 4.5 mm were inserted transarticularly in lag fashion and at disparate angulation [1][13][14][15][16]. To increase stability, the 4.5 mm cortical screws were replaced by 5.5-mm cortical screws [5][15][17][18][19]. Further improvement was achieved through the use of different compression plates [3][15][20][21][22][23]. The system using an axially-positioned narrow locking compression plate (LCP) and 2 abaxial cortical screws has been repeatedly published in recent years and is now regarded as the gold standard [4][8][9][10][11][12]. A newly developed system of the same category (ALPS-20, Kyon, Switzerland) is made of titanium and a titanium alloy instead of steel, and has a different plate and screw design (▶ **Fig. 1**, ▶ **Fig. 2**). In addition to its material properties, other factors that make the ALPS system (ALPS: Advanced Locking Plate System) interesting appealing for use in equine surgery are:

- The plate has particularly limited bone contact, enabling better bone perfusion and therefore fewer disturbances to the microcirculation.
- Specific design and greater diameter of locking screws enable a monocortical placement of the screws, resulting in less tissue damage.

The present study compares the Kyon ALPS-20 system with the Synthes LCP system in an ex vivo experimental setup and focuses on the biomechanics of the constructs as well as the surgical usability in handling the systems. The aim of the mechanical testing is to investigate the 2 PIJ arthrodesis systems in a representative implantation scenario and a physiologically relevant stress situation. In light of the previously described benefits, if the biomechanical stability of ALPS proved to be on par with or superior to that of LCP, then that would be a compelling argument for its consideration and adoption when selecting a plate system for PIJ arthrodesis. It was the null hypothesis (H0) that the 2 systems do not differ in their mechanical capacities.

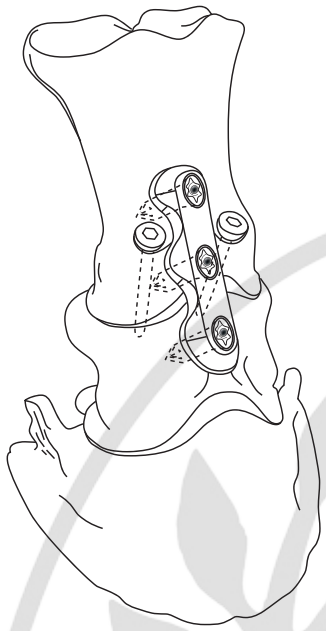

▶ **Fig. 1** Graphic illustration of arthrodesis of the proximal interphalangeal joint using an ALPS-20 plate applied axially in conjunction with 2 abaxial transarticular screws inserted in lag fashion and in converging direction. Source: © A. Vidović.

▶ **Abb. 1** Grafische Darstellung einer Krongelenksarthrodese mit einer axial platzierten ALSP-20-Platte in Kombination mit 2 abaxialen, leicht konvergierenden transartikulären Zugschrauben. Quelle: © A. Vidović.

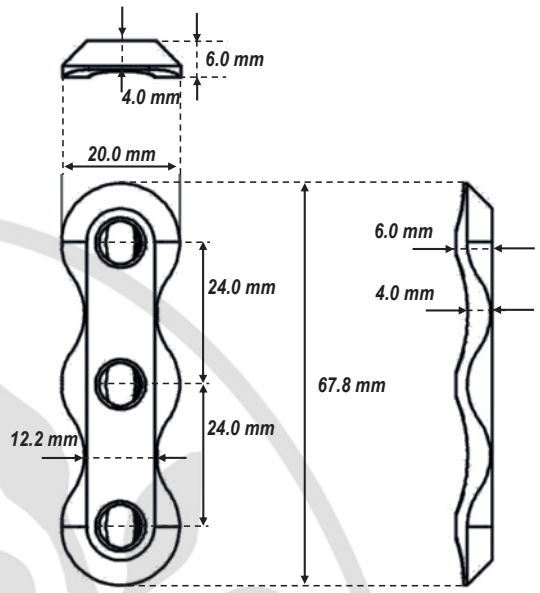

▶ **Fig. 2** Graphic illustration of a 3-hole ALPS-20 plate with indication of measurements. Source: © A. Vidović.

▶ **Abb. 2** Grafische Darstellung der 3-Loch-ALPS-20-Platte mit Maßangaben. Quelle: © A. Vidović.

Materials and methods

Design of experiment

Six pairs of distal limb specimens were prepared for this study (n = 12). The sample size of 6 samples per implant design was determined by a power analysis in OriginLab (Origin Lab Corporation, Northampton, MA, US) for a hypothetical power of 0.9 at a confidence level of 95 % (α = 0.05), based on the preliminary investigations described by Sod et al. [23]. The Kolmogorov-Smirnov test was used to verify a normal distribution for the maximum force, stiffness, and yield point. The measured values were then evaluated for statistical significance ($p < 0.05$) between the 2 plate systems via one-factor ANOVA (Tukey test). The statistical power was verified for yield force, stiffness, and maximum load and the second order error was calculated.

All specimens were derived from Warmblood horses of various ages that were euthanized for non-orthopedic reasons. From each individual horse, either both front legs or both hind legs were dissected at the level of the proximal end of the third metacarpal or metatarsal bone and stored at –22 °C until implantation.

The general surgical handling of the 2 implant systems was evaluated on limb preparations in advance to fully familiarize the operating surgeon, who conducted the ex vivo arthrodesis operations across 2 sessions. Six legs were implanted with the ALPS-20 system on the first day and then 6 legs implanted with the LCP system the following day. For each individual pair of horse limbs, one limb was assigned to System A and the other to System B such that each system was implanted in 3 left and 3 right limb preparations total.

The limb specimens were thawed to room temperature 24 hours before implantation. Limb preparation was conducted identically for both systems. The skin was dissected and removed between the coronary band and the fetlock joint, as well as between the medial and lateral neurovascular bundles. The common extensor tendon was removed between the coronary band and the fetlock joint as well. After incision through the joint capsule and severing of both collateral ligaments, the PIJ was disarticulated. The cartilage layers of both joint surfaces were carefully and completely removed via curette to expose the subchondral bone plate. No reshaping adjustments of the plates to the bone surface were performed in either of the 2 systems.

Technical description of the new ALPS-20

ALPS-20: a locking plate with limited bone contact; width of the plate = 20 mm; total length = 67.8 mm; width at the narrow section between screw holes = 12.2 mm; thickness of the plate = 4 mm; maximum thickness = 6 mm; distance between screw holes = 24 mm; material c. p. (commercially pure) titanium grade 4 (▶ **Fig. 2**). The holes of this plate are designed to accommodate both 6.4-mm locking screws and 4.5-mm cortex screws (in neutral and loaded positions).

Screws: Locking o. d. (outer diameter) 6.4 mm (British Standard Whitworth threads); core diameter = 4.7 mm; material grade 5 titanium-aluminum-vanadium alloy; conventional 4.5-mm c. p. titanium cortical screws.

Handling of the ALPS

The plate was provisionally positioned by hand over the PIJ to determine the position for the transarticular screws. The abaxial entry points for the 2 4.5-mm transarticular screws were marked on the P1 both laterally and medially of the plate at the height between the first and second proximal plate holes (▶ **Fig. 1**). Then 2 glide holes were drilled into the bone using a 4.5-mm drill bit in the direction of the most distal point of the pastern joint surface at the uncovered joint. The glide holes were angled toward one another in a slightly convergent relationship toward the articular surface.

The P1 and P2 were then brought into their physiological position. The drill sleeve was set into the glide hole and with the aid of a 3.2-mm drill bit, the screw holes were drilled transarticularly into the palmar/plantar cortex of the P2 from the glide holes on the P1.

The recesses for the screw heads were prepared with the countersink. Following depth measurement, the 4.5-mm screws were inserted transarticularly and tightened manually in lag fashion, according to touch. In this study, self-tapping 4.5-mm stainless-steel cortical screws were used for both the ALPS and LCP systems.

The 3-hole ALPS-20 was placed dorsally and centrally between the transarticular screws. A 3.2-mm drill bit was used to create a pilot hole in the P2 at a right angle to the distal plate hole, followed by a 5.0-mm drill bit. Maintaining this orientation (perpendicular to the plate) during drilling was facilitated by a 90° drill guide that had been screwed into the plate hole. A self-tapping B-6.4-mm locking screw was then gently placed into the internal thread of the distal plate hole with a single turn. With this system, the screw thread interlocks with the internal thread of the plate from the very start of insertion. The plate and leg specimen were then pressed firmly together with bone tongs and the screw twisted into the P2. As such, the distance between the plate and bones did not change while the screw was being fully tightened. Following the manufacturer's instructions, the screw could easily be screwed to 3.5 Newton meters (Nm) using a torque screwdriver (Torx T30).

A 4.5-mm cortex screw was placed bicortically through the middle plate hole in the loaded (dynamic) position using a 3.2-mm drill bit, and tightened to secure the plate to the P1. A second self-tapping B-6.4-mm locking screw was placed through the proximal plate hole and tightened to 3.5 Nm. Finally, the 4.5-mm cortex screw in the middle plate hole was replaced by a third 6.4-mm monocortical locking screw. The 6.4-mm locking screws used here all had a uniform length of 28 mm and were placed monocortically.

Handling of the LCP

The LCP was initially placed over the PIJ. The entry points for the 2 4.5-mm stainless-steel cortical screws were marked abaxially, laterally, and medially on the P1 at the height of the middle plate hole. The implantation procedure for the 2 transarticular converging compression screws was carried out using the same protocol as for the ALPS.

The LCP plate was then placed centrally between the 2 transarticular screws and fixed to the bone surface with forceps. The 90° drill guide was screwed into the distal plate hole and a 4.3-mm wide hole was drilled into the P2 at right angles bicortically. Following depth measurement, the first self-tapping 5.0-mm locking screw was inserted.

A 4.5-mm cortical screw was inserted into the P1 in the dynamic (loaded) position via the middle plate hole and tightened. Subsequently, a 5.0-mm locking screw of appropriate length was placed in the proximal plate hole and fixed at 4.0 Nm.

In this system, all plate screws were placed bicortically and tightened using 4.0 Nm of force; the screwdriver's torque limiter prevents any excessive force from reaching the screw head.

Radiological and CT imaging of specimens

The position of the implants for both systems was documented radiologically immediately after implantation using 0° and 90° beam paths. Afterwards, all of the specimens were stored covered by plastic wrap in freezer bags at –22 °C until CT examination and evaluation in the biomechanical laboratory.

CT examinations were conducted identically for all sample preparations. All bone implant systems were thawed for 48 hours at 5° C and subsequently stored at 22° C for 2 hours before starting the first CT scan. The first CT scan documented the specimens following implantation. The second CT scan took place after mechanical testing. The primary goal of CT examination was to calculate the deformation of the plate and screws. Additionally, the CT scans should display any bone fractures or implant ruptures, which provides additional information regarding the stability of that particular bone-implant construct.

CT examination was performed using a Philips Mx 8000 IDT 16 CT Scanner (Philips GmbH, Hamburg, Germany). A scout image was made at 120 kV and 50 mAs. The limbs were scanned in a helical fashion, moving from proximal to distal. The acquisition settings were for bone tissue (window width 2000 and window center 500) based on a slice thickness of 1 mm and matrix size of 512 (matrix 512 × 512).

For each preparation, representative CT images in the sagittal plane were selected for measuring deformation. Measurements were made with a picture archiving and editing program (dicomPACS®vet, Oehm and Rehbein GmbH, Rostock, Germany). Plate deformation was defined as the degree of plate bending.

For the deformation measurement, lines were drawn along the longitudinal axis of the plate starting in each case from the distal and proximal end of the plate and continuing over the plate contour exactly in the middle, toward the opposite end. From the intersection of the 2 drawn lines, the program calculated the respective angles. Most plates were bent at only one point (mid plate screw location). With 2 plates that were completely deformed, the angle measurement could not be reliably performed.

Biomechanical testing

For biomechanical evaluation of joint stabilization, uniaxial load displacement measurement was conducted in combination with local 3 D deformation measurement of the implanted plate systems. This required sufficient exposure of the region of interest, priming of the surface in white, and spraying on a stochastic pattern with graphite. For a quasi-static load analysis, the third metacarpal bone, superficial digital flexor tendon, and deep digital flexor tendon were fixed in a hollow cylindrical mounting clamp (inner diameter 70 mm, depth 80 mm) by 4 pairs of orthogonally arranged screws. The remaining volume inside the mounting clamp was filled with water and then cooled over a period of 2 minutes with liquid nitrogen. As

such, a cohesive, solid connection between the specimen and ice was created (Young's modulus of E = 10 N/mm²; tensile strength of σb = 5–10 MPa) [24]. For the duration of the experiment, the temperature was kept well below –70 °C. Steel clips prevented any detached pieces of ice from falling out of the mounting clamp.

The hoof was fixed in a normal position on a 3-sided base to prevent slipping, as shown in ▶ **Fig. 3a**. This kind of clamping allows free rotational movement between the third metacarpal bone/P1 and P2/P3. Moreover, by using this construction a typical physiological loading of the superficial digital flexor tendon and the deep digital flexor tendon could be emulated (▶ **Fig. 3b**). The load was applied a single time axially to the third metacarpal/third metatarsal bone under position control with a test speed of 50 mm/s and up to a maximum displacement of 80 mm using a uniaxial servo-hydraulic testing machine (Instron, Boston, MA, USA).

The force was recorded by a 250 kN load cell using a frequency of 1000 Hz (Instron). Two high-speed cameras (ARAMIS HS 1280 × 1024 pixel) oriented at a 30° angle relative to the specimen recorded 970 frames/second for the entire duration of the test period. Load cell and 3 D measurement systems were synchronized by a trigger signal from the testing machine. The software ARAMIS (Gom, Braunschweig, Germany) was used for displacement analysis of the 2 implant systems.

Statistical data analysis

The maximum force, stiffness, and yield point were determined from the recorded load displacement curves. The first local maximum is referred to as a yield point. The stiffness was determined by means of unweighted linear regression of all measurement points up to the yield point. The Kolmogorov-Smirnov test was used to verify a normal distribution for the maximum force, stiffness, and yield point. The measured values were then evaluated for statistical significance ($p < 0.05$) between the 2 plate systems via one-factor ANOVA (Tukey test). The statistical power was verified for yield force, stiffness, and maximum load and the second order error was calculated.

Results

System implementation

Both systems were used according to the manufacturer's instructions.

The ALPS could be successfully implanted in all cases without any modifications or deviations from the manufacturer's protocol. The self-tapping titanium screws, which are guided by the internal thread of the plate from the very start of insertion, can be easily recessed and facilitate the application of the ALPS.

The LCP system also could be successfully implanted according to the manufacturer's specifications with only minor modifications needed because screwing the self-tapping 5.0-mm locking screws proved difficult for both the P2 and P1. The torque limiter in the screwdriver accompanying the system repeatedly failed to fully insert and tighten the screws using the preset of 4.0 Nm. As such, screws could only be fully locked into place using a backward and forward screwing technique of repeated tightening, loosening, and retightening. When attempting to lock the screw heads into the plate, the prescribed 4.0 Nm of force was not always sufficient, although reliable locking of the screws was always achieved using the method described above. When using the LCP system according to the manufacturer's instructions, placing the middle screw as a lag screw led to deformation of the plate by bending it toward the cortical bone (▶ **Table 1**).

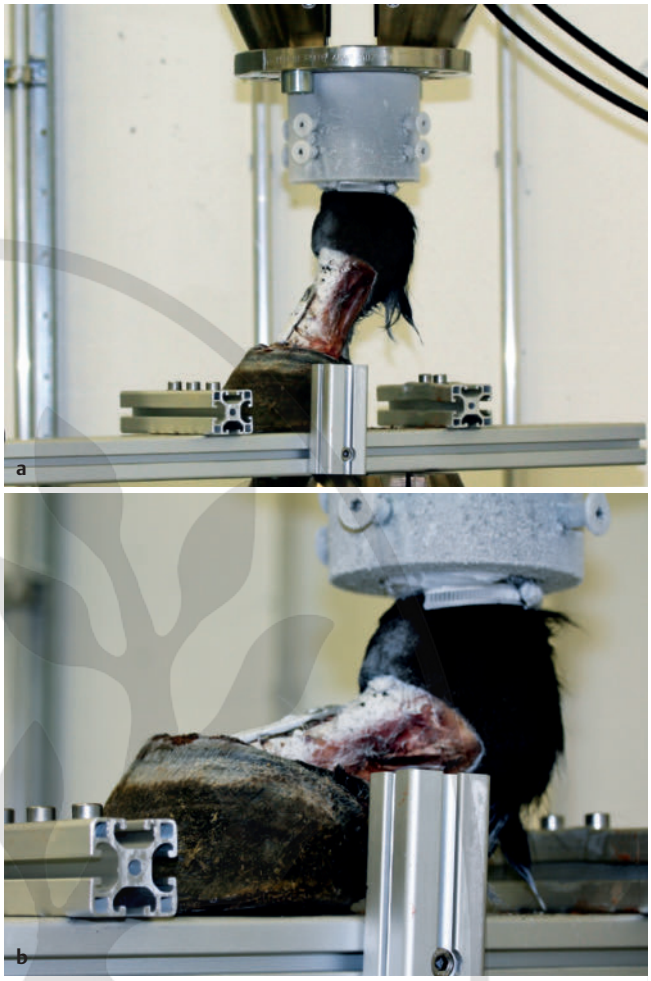

▶ **Fig. 3** Biomechanical testing. **a** For biomechanical testing using a uniaxial servo-hydraulic testing machine, the hoof was fixed in a normal position on a 3-sided base to prevent slipping and rotation. **b** This construction allows typical physiological loading of the limb; under load the fetlock displaces distally. Source: © S. Schwan.

▶ **Abb. 3** Biomechanische Testung. **a** Die biomechanische Testung wurde in einer uniaxialen servohydraulischen Testanlage durchgeführt. Die Zehe ist in physiologischer Stellung, der Huf wurde an 3 Seiten mit Stegen fixiert, um Verrutschen und Rotation zu verhindern. **b** Diese Konstruktion ermöglicht eine nahezu physiologische Bewegung der Gliedmaße. Unter der Belastung verlagert sich das Fesselgelenk nach distal. Quelle: © S. Schwan.

Implant deformation

The ALPS system implants showed no signs of deformation, either in the plates or the screws. In contrast, the LCP demonstrated visible deformation, which had already occurred at the time of implantation from the tightening of the middle screw, as well as during the subsequent testing of the implants (▶ **Table 1**).

▶ **Table 1** Results of plate evaluation after implantation and biomechanical loading.

▶ **Tab. 1** Ergebnisse der Plattenbeurteilung nach Implantation und biomechanischer Belastung.

LCP-system				ALPS-20			
Sample number	**Deformation after implantation**	**Deformation after biomechanical test**	**Fissures**	**Sample number**	**Deformation after implantation**	**Deformation after biomechanical test**	**Fissures**
1 L	6.0°	6.3°	Yes	1 R	0°	0°	No
2 L	6.4°	7.0°	No	2 R	0°	0°	Yes
3 L	5.6°	6.2°	Yes	3 R	0°	0°	No
4 L & 4 R	Pilot specimens for adjustment of the biomechanical testing machine						
5 R	6.2°	180° Buckling	Yes	5 L	0°	0°	Yes
6 R	10.0°	Fracture	Yes	6 L	0°	0°	No
7 R	2.3°	3.1°	No	7 L	0°	0°	Yes

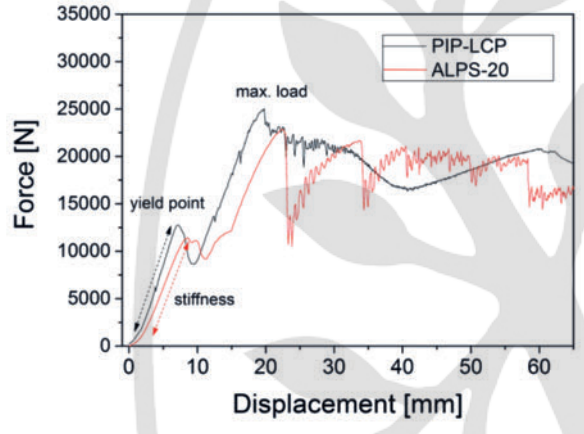

▶ **Fig. 4** Diagram showing a typical force-displacement curve for both implant systems ALPS-20 and LCP. Source: © S. Schwan.

▶ **Abb. 4** Das Diagramm zeigt eine typische Kraft-Verteilungs-Kurve für beide Implantatsysteme (ALPS-20 und LCP). Quelle: © S. Schwan.

CT analysis

After biomechanical testing, deformations ranging between 3.1° and 7.0° were measured in 4 LCPs (▶ **Table 1**). A total implant failure was observed for preparations 5 R and 6 R. The 5 R implant fully collapsed (180° bend) while the 6 R implant broke. A break line extended transversely to the longitudinal axis of the implant and through the middle screw hole. This localization corresponds to the seat of the 4.5-mm cortex screw inserted into this screw hole in the dynamic/loaded position. In addition, the locking screw placed in the proximal screw hole was bent immediately distal to the screw head by 90°. CT examination revealed fissures in various bones (third metacarpal/third metatarsal bone, P1 and P2), at different localizations, and in varying numbers (▶ **Table 1**).

Mechanical stability

The typical force-displacement curve for both implant systems shows a steady course up to the yield point, which occurs at 10 000 to 15 000 N. At the yield point a sudden load drop occurs, indicating the sudden failure of a load-bearing structure (▶ **Fig. 4**). The elongation of both implants, measured by means of ARAMIS, was negligibly small. The force curve then rises once again in similar fashion, and then passes into an irregular curve when the maximum force (20 000 to 25 000 N) is reached (▶ **Fig. 4**).

The values for the mechanical parameters were all normal distributions and did not differ significantly between the 2 implant systems (yield force $p = 0.23$; maximum load $p = 0.91$; stiffness $p = 0.77$). ▶ **Fig. 5** shows the corresponding boxplots. The average yield force was 11 000 N for LCP preparations and 14 000 N for ALPS preparations (▶ **Fig. 5a**). The stiffness of the LCP preparations and the ALPS preparations were roughly the same, at approximately 2500 N/mm^2 (▶ **Fig. 5b**). The maximum load for both preparation groups was about 21 000 N at the same height (▶ **Fig. 5c**).

Discussion

The ex vivo mechanical testing in this study is far superior to 3-point or 4-point bending tests when it comes to simulating the biomechanics of physiological loading in standing limbs [11][12]. Three-point/4-point bending tests predominantly evaluate the material strength of the implant, while neglecting to consider the complex biomechanics in the appropriate anatomic and physiological context. During normal gait, a complex combination of compressive thrust, torsional, and bending forces act on the construct. The simultaneous action of these stresses leads to an overlapping stress state [25] in the implant and bone composite. This complex stress state is responsible for the type of mechanical failure that occurs [30]. In various studies, constructs have been examined by means of 3-point [15][26][27] or 4-point bending tests [8]. These test methods induce a pure bending stress into the composite that does not occur physiologically. As a result of this test method being chosen, the construct can withstand relatively high loads. This resistance is due to the high bending stiffness (titanium with

E = 110 N/mm² or stainless steel with E = 210 N/mm²) of the implant material [28]. Data for speed tests of 1 mm/s [10], 5 mm/s [8] or 19 mm/s [9][26] have been reported for both 3-point and 4-point bending tests. The resulting force-displacement curves are roughly equivalent to those seen in tabulated data for the material (titanium or stainless steel). As such, these constructs and implantation techniques appear to be extremely stable at first glance; however, they ignore the complex movement physiology that impacts implant performance in actual practice. Therefore, the mechanical results determined in the present study are not directly comparable to these other methods that ignore physiology.

In this study, a testing speed of 50 mm/s was chosen, with the intent of realistically approximating the physiological loading speed of a horse limb in situ. This testing speed can also be found in studies by Sod et al. [11][20], where biomechanical testing was used to measure the entire limb. No statistically significant differences between the 2 preparation groups were calculated across all of the measured parameters. As the Kolmogorov-Smirnov test shows, all preparations originate from a normally distributed population. The strain of both implants, measured by means of ARAMIS, was negligibly small and clearly under the elastic limit for steel and titanium [28].

The use of both whole and partial limb preparations leads to the use of test setups that are more likely to accurately represent the true biomechanical situation experienced in situ [11][12] and, as a rule, result in lower values with respect to stiffness and strength. This is because a material composite of implant, bone, and surrounding soft tissue is tested rather than purely the implant material itself. Sod et al. [11] have determined a static yield point at 24.4 ± 2.2 kN as well as a maximum force of 25.7 ± 2.3 kN in studies on the LCP. The value of the yield point in that report is about twice as large as that determined in this study. The method described by Sod et al. [29] uses the entire leg as an implant carrier and introduces the force in the area of the proximal limb. This results in a load distribution and a continuous load reduction over the height of the limbs because the elbow and the carpal joint are compressed. In this case, it is not possible to separate which force acts in the surrounding structures and which acts in the implant. Therefore, a direct comparison of the absolute numbers obtained with these 2 test setups is not realistic.

As shown in our investigations, the first sudden drop in load results from a failure of soft tissue. However, the resistance of soft tissue in this study cannot be compared with an in vivo scenario. In fact, in an ex vivo study any kind of preparation leads to a deviation from the true physiological state. In this study, all legs were severed distal to the carpal or tarsal joints. Thus, all flexor and extensor tendons in the metacarpal or metatarsal region were severed. This results in altered physiological force transmission under axial load during biomechanical testing. Due to the way in which the specimen was fixed with ice, all the "tendon packages" were fixed in a near physiological position on all preparations with the third metacarpal/third metatarsal bone (note: the cut through the bone and the tendons was in the same plane). This arrangement remained undamaged after the test. Although we do not know how much additional stabilization the preparations have received through the fixation technique, the starting point for all preparations was the same; as such, both systems were tested under the same conditions.

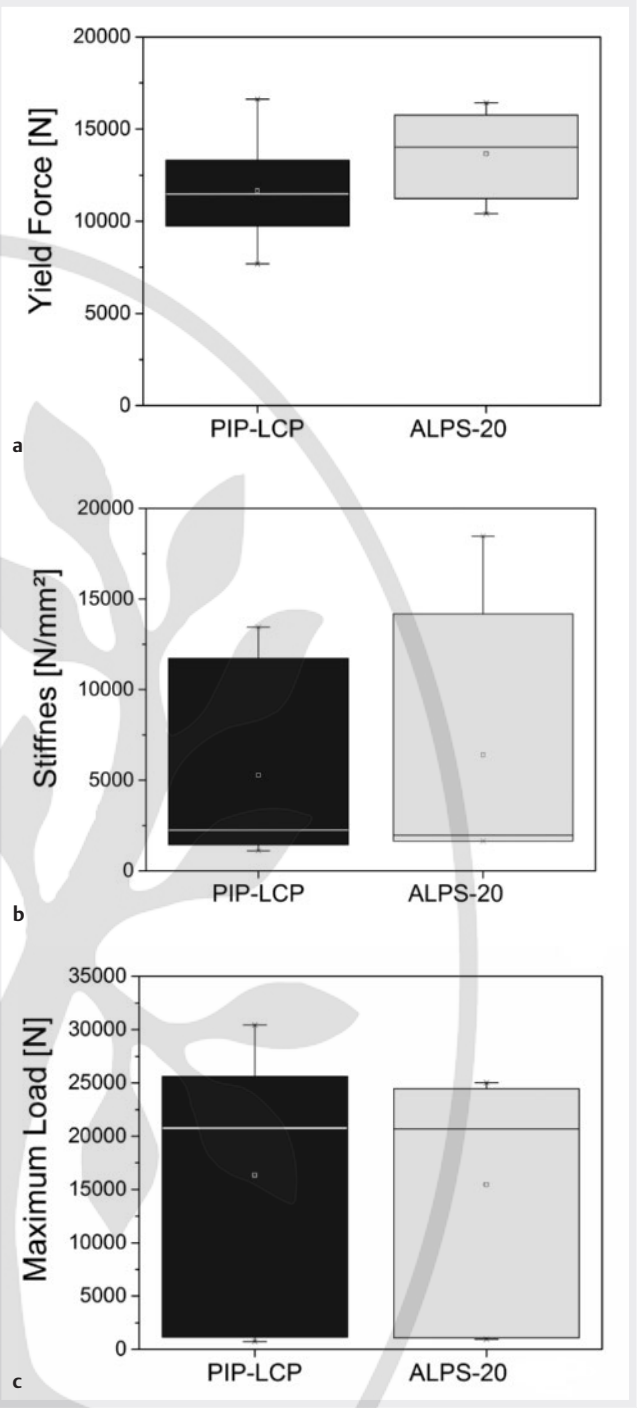

▶ **Fig. 5** The Box-plot diagrams illustrate the mechanical parameters of the 2 implant systems ALPS-20 and LCP for yield force **a**, stiffness **b** and maximum load **c**. Source: © S. Schwan.

▶ **Abb. 5** Die Boxplot-Diagramme zeigen die Werte der untersuchten biomechanischen Parameter der Implantatsysteme ALPS-20 und LCP in Bezug auf Fließpunkt **a**, Steifheit **b** und Maximalbelastung **c**. Quelle: © S. Schwan.

The yield point is associated with a failure of the stabilizing effect of the soft tissue. The soft tissues that play a role in this kind of preparations are the following:

1. The superior digital flexor tendon (SDFT), deep digital flexor tendon (DDFT), inferior check ligament (ICL) in front limbs and suspensory ligament (SL) were severed and recaptured/embedded with ice. The thermal properties of bone (high heat capacity, low heat conduction) [29][30] limit significant cooling of the limb below the clamp over the time interval of sample handling and measurement.
2. The ligaments of the proximal sesamoid bones have a stabilizing effect on an axial load and they remained intact, however their function is partially dependent on an intact SL.
3. The collateral ligaments of the fetlock and coffin joints were undamaged and provide certain stabilization under axial load.
4. The common digital extensor tendon (CDET) and the lateral digital extensor tendon (LDET) were severed proximally with the cannon bone and fixed with ice. They have no stabilizing effect under axial load, however:
5. Due to the removal of the CDET, the 2 branches of the extensor branch of SL were also rendered nonfunctional because they enter the CDET. These ligaments would have a stabilizing effect under axial load.

An additional tissue failure occurs with further loading. In the tests carried out here, mechanical failure of the implants occurred in 2 cases. In one case, plastic deformation of the plate led to a complete fracture. Based on the CT scans taken after the mechanical test, there was no visible displacement of the screws or plate in any of the other implants. In these preparations, the implants withstood the applied force; however, osseous changes did occur in 7 of the 12 preparations (▶ **Table 1**). Via CT evaluation, fissures were found in various bones at different localizations, and in varying numbers. The fissures arose after biomechanical testing. The impact of freezing on fissure formation cannot be definitively excluded, but is presumably not substantial. The first CT examination took place after thawing the preparations and before biomechanical testing. No fissures were detected at that time. Afterwards the preparations were tested and reexamined by CT. During this interim, the preparations were not refrozen. However, no statement can be made as to whether the bone fissures originated in association with the implants or solely because of the force applied during biomechanical testing.

The design of ALPS is very different in many ways compared to LCP. As such, a further aim of the study was to compare the surgical usability in handling both of the plate systems. In particular, the following points were noted:

1. Due to the use of lighter materials, the indented shape, the rougher texture, as well as the construction of the ventral surface, the ALPS plate was easier to handle and slipped less during positioning.
2. The novel screw guidance and locking system of the ALPS, in which the screw is guided in the threaded hole of the plate from the outset, proved to be easier when placing screws. According to ALPS product information, the insertion (tapping) torque in these new locking screws is reduced 2-fold. In the course of this study, we found that with ALPS it is easier for the screws to pass through the bone, as well as the subsequent locking of the plate-bone system also being substantially easier. The screws on ALPS could easily be tapped and tightened with only 3.5 Nm and locked in place, despite being 1.4 mm thicker than those of the LCP.
3. The implantation of the uniform-length 28 mm monocortical B-6.4-mm screws was quicker, did not require accounting for screws of varying length, and minimized the surgery-induced trauma to only one bone cortex. On the other hand, correct transcortical application of the LCP system requires different lengths of both cortical screws and locking screws to be accounted for at the same time.
4. The term “limited bone contact plate” is more applicable to the ALPS plate than the LCP. While the LCP is in contact with the bone over a limited area, the ALPS plate only touches the bone to the left and right of each screw hole.

The manufacturer’s recommendation for large-area systems is to tighten the 5.0-mm locking screws with a defined force of 4.0 Nm by using a torque limiter. Similar data is also found in studies by Sod et al. [11] and Rocconi et al. [9]. While this torque allowed all screws to be rotated through the cis cortex, most screws remained stuck in the transcortical plane because the torque limiter triggered at 4.0 Nm. As such, the screws could only be fully embedded by repeated forward and backward rotation. This circumstance also made locking the screws into the plate more difficult. We believe that this problem would be solved by the use of a thread cutter, which was not available for the LCP screws. Zoppa et al. [12] used a screwdriver with a torque limiter of 8.0 Nm. It remains unclear whether the manufacturer recommends 2 different tool settings with the same plate system. It is clear from our experience, however, that 4.0 Nm of torque is insufficient for securing the self-tapping 5.0-mm locking screws into the horse limb, and increasing the torque to 8.0 Nm would likely be more suitable.

In the current literature, a parallel or slightly divergent orientation is recommended for transarticular cortical screws. From personal clinical experience, the authors prefer a slightly convergent orientation for transarticular screws. Because this placement was applied equally to both systems, it should not impact the comparability for this study.

Biomechanical evaluation has demonstrated that both of the tested systems ensure a very secure and resilient connection between the P1 and P2. This study does not provide any information about the behavior of the implants under long-term cyclic loading. This is therefore a first approach to compare the 2 systems and should be followed, as is conventional, by further scientific evaluation under different experimental conditions.

CONCLUSION FOR PRACTICE

The aim of the study was to compare the mechanical stability and the surgical usability in handling of 2 different LCP-Systems. The Kyon ALPS-20 system demonstrates comparable mechanical properties to the Synthes LCP in the present study’s ex vivo test model for equine PIJ arthrodesis. As such, the Kyon ALPS-20 may be a good alternative to the Synthes LCP for equine proximal interphalangeal joint.

Disclosures

The authors declare that the research was conducted in the absence of any commercial or financial relationships that could be construed as a potential conflict of interest.

Data availability

The datasets generated for this study are available upon request to the corresponding author.

Author contribution

AV contributed to study conception and design, specimen preparation, data collection, and manuscript preparation. DJ contributed to manuscript editing and literature research. SS performed the statistical analysis and AG designed mechanical testing. CL contributed to manuscript writing and editing. WB contributed to study design and data collection in the biomechanical laboratory, as well as manuscript editing. All authors contributed to manuscript revision.

Acknowledgements

We would like to thank Dr. Kerstin Gerlach for their help and performance of CT scans and evaluations. We would also like to acknowledge the Equine Clinic Burg Müggenhausen for providing the implants for this study.

References

[1] Caron JP, Fretz PB, Bailey JV et al. Proximal interphalangeal arthrodesis in the horse – a retrospective study and a modified screw technique. Vet Surg 1990; 19 (3): 196–202 doi:10.1111/j.1532-950X.1990.tb01167.x

[2] Herthel TD, Rick MC, Judy CE et al. Retrospective analysis of factors associated with outcome of proximal interphalangeal joint arthrodesis in 82 horses including Warmblood and Thoroughbred sport horses and Quarter Horses (1992–2014). Equine Vet J 2016; 48 (5): 557–564. doi:10.1111/evj.12503

[3] Knox PM, Watkins JP. Proximal interphalangeal joint arthrodesis using a combination plate-screw technique in 53 horses (1994–2003). Equine Vet J 2006; 38 (6): 538–542. doi:10.2746/042516406X154840

[4] Lischer CJ, Auer JA. Arthrodesis techniques. In: Auer JA, Stick JA, eds. Equine Surgery. 4th ed. St. Louis: Saunders; 2012:1130–1147. doi:https://doi.org/10.1016/B978-1-4377-0867-7.00081-8

[5] MacLellan KNM, Crawford WH, MacDonald DG. Proximal interphalangeal joint arthrodesis in 34 horses using two parallel 5.5-mm cortical bone screws. Vet Surg 2001; 30 (5): 454–459. doi:10.1053/jvet.2001.25873

[6] Schaer TP, Bramlage LR, Embertson RM et al. Proximal interphalangeal arthrodesis in 22 horses. Equine Vet J 2001; 33 (4): 360–365. Available at: http://www.scopus.com/inward/record.uri. doi:10.2746/042516401776249552

[7] Auer JA. Proximal interphalangeal arthrodesis: screw fixation. In: Fackelman GE, Auer JA, Nunamaker DM, eds. AO Principles of Equine Osteosynthesis. Davos Platz, Switzerland: AO Publishing/Thieme Verlag; 2000: 221–231

[8] Ahern BJ, Showalter BL, Elliott DM et al. In vitro biomechanical comparison of a 4.5 mm narrow locking compression plate construct versus a 4.5 mm limited contact dynamic compression plate construct for arthrodesis of the equine proximal interphalangeal joint. Vet Surg 2013; 42 (3): 335–339. doi:10.1111/j.1532-950X.2013.01111.x

[9] Rocconi RA, Carmalt JL, Sampson SN et al. Comparison of limited-contact dynamic compression plate and locking compression plate constructs for proximal interphalangeal joint arthrodesis in the horse. Can Vet J 2015; 56 (6):615–619

[10] Seo J, Yamaga T, Tsuzuki N et al. In vitro biomechanical comparison of a 5-hole 4.5 mm locking compression plate and 5-hole 4.5 mm dynamic compression plate for equine proximal interphalangeal joint arthrodesis. Vet Surg 2014; 43 (5): 606–611. doi:10.1111/j.1532-950X.2014.12164.x

[11] Sod GA, Riggs LM, Mitchell CF et al. A mechanical comparison of equine proximal interphalangeal joint arthrodesis techniques: An axial locking compression plate and two abaxial transarticular cortical screws versus an axial dynamic compression plate and two abaxial transarticular cortical screws. Vet Surg 2011; 40 (5): 571–578. doi:10.1111/j.1532-950X.2011.00830

[12] Zoppa ALV, Santoni B, Puttlitz CM et al. Arthrodesis of the equine proximal interphalangeal joint: A biomechanical comparison of 3-hole 4.5 mm locking compression plate and 3-hole 4.5 mm narrow dynamic compression plate, with two transarticular 5.5 mm cortex screws. Vet Surg 2011; 40 (2): 253–259. doi:10.1111/j.1532-950X.2010.00792.x

[13] Genetzky RM, Schneider EJ, Bulter HC et al. Comparison of two surgical procedures for arthrodesis of the proximal interphalangeal joint in horses. J Am Vet Med Assoc 1981; 179 (5): 464–468

[14] Steenhaut M, Verschooten F, Demoor A. Arthrodesis of the pastern joint in the horse. Equine Vet J 1985; 17 (1): 35–40

[15] Watt BC, Edwards RB, Markel MD et al. Arthrodesis of the equine proximal interphalangeal joint: A biomechanical comparison of three 4.5-mm and two 5.5-mm cortical screws. Vet Surg 2001; 30 (3). doi:10.1053/jvet.2001.23353

[16] Zamos DT, Honnas CM. Principles and Applications of Arthrodesis in Horses. Comp Contin Educ Pract Vet 1993; 15 (11):1533–1541

[17] Carmalt JL, Delaney L, Wilson DG. Arthrodesis of the proximal interphalangeal joint in the horse: A cyclic biomechanical comparison of two and three parallel cortical screws inserted in lag fashion. Vet Surg 2010; 39 (1): 91–94. doi:10.1111/j.1532-950X.2009.00614.x

[18] Read EK, Chandler D, Wilson DG. Arthrodesis of the equine proximal interphalangeal joint: A mechanical comparison of 2 parallel 5.5 mm cortical screws and 3 parallel 5.5 mm cortical screws. Vet Surg 2005; 34 (2): 142–147. doi:10.1111/j.1532-950X.2005.00022.x

[19] Schneider RK, Bramlage LR, Hardy J. Arthrodesis of the distal interphalangeal joint in 2 horses using 3 parallel 5.5-mm cortical screws. Vet Surg 1993; 22 (2): 122–128. doi:10.1111/j.1532-950X.1993.tb01685.x

[20] Sod GA, Riggs LM, Mitchell CF et al. An in vitro biomechanical comparison of equine proximal interphalangeal joint arthrodesis techniques: An axial positioned dynamic compression plate and two abaxial transarticular cortical screws inserted in lag fashion versus three parallel transarticular cortical screws inserted in lag fashion. Vet Surg 2010; 39 (1): 83–90. doi:10.1111/j.1532-950X.2009.00615.x

[21] Galuppo LD, Stover SM, Willits NH. A biomechanical comparison of double-plate and Y-plate fixation for comminuted equine second phalangeal fractures. Vet Surg 2000; 29 (2). doi:10.1111/j.1532-950X.2000.00152.x

[22] James FM, Richardson DW. Minimally invasive plate fixation of lower limb injury in horses: 32 cases (1999–2003). Equine Vet J 2006; 38 (3): 246–251. doi:10.2746/042516406776866291

[23] Sod GA, Mitchell CF, Hubert JD et al. In vitro biomechanical comparison of equine proximal interphalangeal joint arthrodesis techniques: Prototype equine spoon plate versus axially positioned dynamic compression plate and two abaxial transarticular cortical screws inserted in lag fashion. Vet Surg 2007; 36 (8). doi:10.1111/j.1532-950X.2007.00338.x

[24] Scapozza C. Entwicklung eines dichte- und temperaturabhängigen Stoffgesetzes zur Beschreibung des visko-elastischen Verhaltens von Schnee. Zurich, Swiss Federal Institute for Technology, 2004

[25] Kolupaev VA, Yu M-H, Altenbach H. Fitting of the strength hypotheses. Acta Mechanica 2016; 227 (6): 1533–1556. doi:10.1007/s00707-016-1566-9

[26] Bras JJ, Lillich JD, Beard WL et al. Effect of a collateral ligament sparing surgical approach on mechanical properties of equine proximal interphalangeal joint arthrodesis constructs. Vet Surg 2011; 40 (1): 73–81. doi:10.1111/j.1532-950X.2010.00741.x

[27] Wolker RRE, Wilson DG, Allen AL et al. Evaluation of ethyl alcohol for use in a minimally invasive technique for equine proximal interphalangeal joint arthrodesis. Vet Surg 2011; 40 (3): 291–298. doi:10.1111/j.1532-950X.2010.00794.x

[28] Wintermantel E, Ha S-W. Medizintechnik Life Science Engineering. Berlin: Springer; 2008. https://www.springer.com/de/book/9783540939351

[29] Biyikli S, Modest MF, Tarr R. Measurement of thermal properties for human femora. J Biomed Mat Res 1986; 20 (9): 1335–1345

[30] Calttenburg R, Cohen J, Conner S et al. Thermal properties of cancellous bone. J Biomed Mat Res 1975; 9 (2):169–182